Exploring original properties of GaN-BN alloys using high-throughput ab initio computation

H. Maiz Hadj Ahmed, H. Benaissa, Ali Zaoui, M. Ferhat

Version of Record: https://www.sciencedirect.com/science/article/pii/S0030402622005228
Manuscript_4962a9c96bb9032166c48128c4448c52

Exploring original properties of GaN-BN alloys using high-throughput *ab initio* computation

H. Maiz Hadj Ahmed[1], H. Benaissa[1], A. Zaoui[2,*] and M. Ferhat[1]

[1]*Département de Génie Physique, (LPMF). Université des Sciences et de la Technologie d'Oran, Mohamed Boudiaf. Oran, Algeria*

[2]*Univ. Lille, IMT Lille Douai, Univ. Artois, JUNIA, ULR 4515 - LGCgE, Laboratoire de Génie Civil et géo-Environnement, F-59000 Lille, France*

ABSTRACT

GaN alloyed with boron (B) is a potential candidate for wide band gap materials and for ultraviolet optoelectronic device applications. Using evolutionary algorithm and density functional theory, we investigate here the thermodynamic, mechanical, dynamical and optical properties of GaN-BN alloys. Three ordered $B_xGa_{1-x}N$ structures: cubic (BGa_3N_4, and B_3GaN_4, space group *P*-43m), and tetragonal ($BGaN_2$, space group *P*-42m) have been explored. The calculated relatively large mixing enthalpies point out that large miscibility gap exists in BGaN system (i.e., ΔH~80meV for x=0.5). However, weak ΔH for x = 0.25 (ΔH~24meV) suggests that BGa_3N_4 compound is –thermodynamically- slightly unstable. Analysis of the computed elastic constants and phonon dispersion curves reveal that the three ordered structures are mechanically and dynamically stable. Our results show that BGa_3N_4 exhibits outstanding mechanical properties, such as a large bulk modulus (~328GPa), important shear modulus (~248GPa), and strong Vickers hardness of ~ 33GPa. Moreover, the use of LDA-1/2 functional evidences that the incorporation of boron in GaN gives a huge optical band-gap bowing parameter of b~11eV for the entire range of composition, which is in agreement with experiment. In addition, we highlight the prevailing role of chemical and stress effects responsible of the giant disorder in this ternary system.

Keywords: *GaN-BN alloys; high-throughput computations; DFT; band-gap; bowing parameter.*

*Email address: azaoui@polytech-lille.fr

1 Introduction

Recently, an increasing attention has been paid to semiconductor alloys due to their various applications, particularly in the fields of electronics and optoelectronics. For instance, the case of nitride III semiconductor alloys, such as InGaN and AlGaN, which have particularly revolutionized the lighting industry and thus opened the way for diodes [1-3]. Efficient, visible and ultraviolet (UV) light-emitting diodes (LEDs) are currently becoming the best alternative for future lighting applications. These applications also offer the possibility to get significant energy savings that exceed those of conventional light sources.

While III-V-N alloys (AlGaN, InGaN, AlInN) have been studied intensively, research involving ternary alloys based on nitride of common anions such as $B_xGa_{1-x}N$ is still in its beginning. In principle, the boron alloy in wurtzite GaN offers a particular opportunity concerning the possibility of increasing the band-gap of GaN of the blue spectral region to UV. Wurtzite BGaN alloys have been the subject of several experimental studies [1-7]; and their corresponding electronic structures were investigated theoretically in Refs. [8-10].

Recently, Maiz Hadj Ahmed et al. have investigated BN-AlN alloys by combing density functional theory and evolutionary structure predictions [11]. They predicted three compounds (cubic (BAl_3N_4, and B_3AlN_4, space group *P*-43m), and tetragonal ($BAlN_2$, space group *P*-42m)). They have also shown that the direct band gap of BN-AlN evinces strong deviation from a linear dependence on B composition. A giant direct band gap bowing parameter of b~11.6eV was obtained for the entire range of composition, where b parameter was found to be sensitive to composition x and comes mainly from structural and chemical contributions.

For optoelectronic devices, the evolution of the direct energy gap Eg(x) with composition x, have been a significant challenge in materials theory. However, the change of Eg(x) splits from the linear interpolation between components of band-gaps of the alloyed compounds, i.e., Vegard's linear 'law' (known as the virtual crystal approximation (VCA)). However, displayed simple quadratic function on composition x unmasks a bowing parameter b. A number of different models have been proposed to describe the band gap bowing through the knowledge of the band-gap variation.

The earliest models were mainly based on the VCA; while modern approach uses large supercells to treat the alloys. Methods such as VCA seems to be inadequate in such cases, since chemical and structural effects are not taken into account [12]. However, the second approach has been successfully applied to describe accurately semiconductors alloys [13-18] but needs massive computational efforts [13-18].

In this paper we carry out novel theoretical approach based on the recently developed evolutionary algorithm within the density functional theory (DFT) in order to describe accurately the band-gap dependence on B composition in $B_xGa_{1-x}N$ alloys. New phase structures are explored, and a special attention is paid to the study of the band-gap dependence and the optical band-gap bowing parameter of this ternary system.

2 Method

In order to fix the most stable and low enthalpy structures of GaN-BN alloys, we use an evolutionary algorithm approach as implemented in Material project database [19-20]. The first-principles electronic structure calculations were achieved in the framework of density functional theory (DFT) [21] using a plane-wave basis set. The computed total-energy was carried out by the Quantum ESPRESSO Package code [22]. The exchange-correlation term was approximated by the linearized density approximation (LDA) [23]. The interactions between the ions and electrons are described here by the projector-augmented wave pseudopotential scheme (PAW) [24], with a cut-off of 65 Ry. An energy cut-off of 600 Ry was included for the charge density. The calculations were performed with dense Monkhorst-Pack [MP] [25] *k*-points mesh of 10×10×8 for $BGaN_2$ and 12×12×12 for BGa_3N_4 and B_3GaN_4 respectively. The phonon properties were obtained by means of the density functional perturbation theory (DFTP) [26]. A 6 × 6 × 3, 4 × 4 × 4, and 4 ×4 × 4 *q*-points MP mesh has been used to perform inverse Fourier transformation for $BGaN_2$, BGa_3N_4, and B_3GaN_4 respectively. These settings ensure convergence of total energies to within 1meV per atom. Structure relaxation proceeded until all forces on atoms were less than 1meV/Å.

3 Results and Discussion

Structural properties

The analysis of the high-throughput search gives three main candidate phases of $B_xGa_{1-x}N$ alloys: BGa_3N_4 (x = 0.25, cubic phase, space group P-43m), $BGaN_2$ (x = 0.5, tetragonal phase, space group P-4m2), and B_3GaN_4 (x = 0.75, cubic phase, space group P-43m). The predicted structures, corresponding structural findings, are listed in Table I.

The calculated lattice constant a, and c/a ratio of wurtzite (WZ) GaN and BN agree well with experimental measurements. Let us underline here that the calculated lattice constants are slightly weaker than the experimental values, as found previously in most LDA calculations.

Thermodynamic properties and phase stability

In order to assess the thermodynamic stability/instability of $B_xGa_{1-x}N$ alloys, we check out the formation enthalpy, which is defined as:

$$\Delta H = E(x) - (1-x)\, E(\mathrm{GaN}) - x\, E(\mathrm{BN})$$

Where $E(x)$ is the total energy of the alloy at composition x, and E(GaN) and E(BN) are the total energy of WZ GaN and BN respectively. Fig. 1 displays the alloy formation enthalpy ΔH. The positive sign of ΔH points that the ground state of these alloys at T = 0K corresponds to a propensity to phase separation into pure WZ constituents GaN and BN. The magnitude of ΔH is relatively marked for x = 0.5 (ΔH = 80meV), which reflects large miscibility gap. Nevertheless, the magnitude of the mixing enthalpy for x = 0.25 is relatively weak (ΔH = 24meV), the ordered phase BGa_3N_4 has a much lower ΔH compared to $BGaN_2$, suggesting that BGa_3N_4 alloy is -to some extent- insignificantly unstable with respect to WZ binary compounds GaN and BN.

Mechanical properties

The calculated elastic constants C_{ij} of wurtzite GaN and BN compounds and BGaN alloys are presented in Table II. The WZ phase of BN and GaN, which have a stable phase at room temperature, meet the mechanical stability criteria. Furthermore, the calculated elastic constants of BGa_3N_4, $BGaN_2$, and B_3GaN_4 compounds meet the Born stability criteria.

The bulk modulus (B_0) obtained from the elastic constants, shear moduls (G), Young's modulus (E) and Poisson's ratio (ν) are given in Table III. Among, the $B_xGa_{1-x}N$ ordered

structures, B_3GaN_4 has the largest B_0 of 328GPa, which can be comparable with many transition metal nitrides, such as OsN_2 (B_0 = 353GPa), and IrN_2 (B_0 = 333GPa). The shear modulus measures to the shape change at constant volume offers a high correlation with hardness than bulk modulus. Again, excluding BN, B_3GaN_4 has the largest shear modulus of 248GPa.

However, it is widely consented that large bulk and shear moduli do not warrant at all high hardness of a material. Thus, qualitative estimation for a macroscopic model is necessary. We evaluate the Vickers hardness of BGa_3N_4, $BGaN_2$, and B_3GaN_4 compounds using Chen's model [27] according to:

$$H_v = 2(\kappa^2 G)^{0.585}-3$$

where κ is the Pugh ratio, $\kappa = G/B$. We found a Vickers hardness of 17.5GPa, 22.01GPa and 33.28GPa for BGa_3N_4, $BGaN_2$, and B_3GaN_4 respectively, which show that B_3GaN_4 is the hardest material among the GaN-BN system, confirming -hence- the excellent hardness of ~33GPa.

Dynamical properties

To study the dynamical stability of cubic (BGa_3N_4, and B_3GaN_4) and tetragonal ($BGaN_2$) phases of BGaN alloys, the phonon properties are investigated. The calculated phonon dispersion curves along the high-symmetry lines are illustrated in Fig. 2. All the frequencies are real, i.e., no imaginary phonon frequencies are revealed overall the Brillouin zone for all phases, which confirms the dynamical stability of BGa_3N_4, $BGaN_2$ and B_3GaN_4 ordered structures of BGaN.

Optical properties

Let us focus here on the evolution of the band-gap of $B_xGa_{1-x}N$ with the variation concentration x of B. It is well known that the band-gap formation can be only faultlessly described within a many-body theory. This takes appropriately into account the electron-hole excitations, since standard DFT underestimates seriously band-gap by 50% to 100%. Therefore, we used here the LDA-1/2 technique [33], which compete well with the most popular many-body GW quasiparticle approach [34]. For WZ-GaN, the calculated fundamental gap ($\Gamma \rightarrow \Gamma$) of 3.5 eV is in excellent agreement with reported experimental value

of 3.507eV [28]. However, for WZ-BN, the obtained direct (Γ→Γ) and indirect (Γ→K) band gaps are 10eV and 7.18eV respectively. To the best of our knowledge, no experimental data are available for wurtzite BN. Nevertheless, the computed indirect band-gap of WZ BN is widely close to GW calculations of 6.86eV [35] and scissors operator method of 6.8eV [35].
The composition dependence as function of composition for the direct band-gap $E_g(x)$ of $B_xGa_{1-x}N$ alloys is shown in Fig. 3. The nonlinear dependence of $E_g(x)$ on the B composition can be expressed by the standard bowing equation:

$$E_g(x) = (1-x)\, E_g(GaN) - x\, E_g(BN) - b\, x\, (1-x)$$

Where b stands for the optical band gap bowing parameter. $E_g(x)$ shows an important disparity from the linear interpolation, i.e., from the Vegard's law shown by the dashed line, which rule out any bowing. From least-squares fit we calculated band gaps $E_g(x)$ (solid circles), which yields a giant optical band-gap bowing parameter b of 10.96eV for the entire range of alloy boron composition x. The obtained huge b is in contrast with conventional III-V semiconductors alloys such as AlGaSb (b~0.1eV) [12] and InPAs (b~0.14eV) [12], where b is relatively weak and composition-independent. Moreover, the bowing parameter b of GaN-BN system is quite comparable to many III-V-N mixed anions alloys such as GaAsN (b~7.5eV) [12], GaPN (b~9.5eV) [37] and boron-based III-V ternary alloys, such as BNAs (b~12.3eV) [38], BInN (b~13.5eV) [38], and BAlN (b~8.55eV) [39]. Our calculated optical bowing is much larger than the calculated (b~4.3eV) of Escalanti et al. [8] but agrees with our calculated bowing derived from a phenomenological model (b~7.3eV) [38]. More importantly our present calculated band-gap bowing agrees with the recent photoluminescence measurement (b~9.2±0.5eV)[5]. To origin of the nonlinearity of the band gap via the optical band-gap bowing parameter b mainly comes from two different physical effects, namely structural (or geometric) quantified by b_{VD} and b_{SR}, and chemical (or electronic) effect quantified by b_{CE}. Zunger and co-workers [40] have proposed a three-step process to transform the binary compounds GaN and BN into the ternary BGaN alloys. (i) In the VD process (volume deformation effect), we compress GaN and dilate BN from their equilibrium volume to alloy $V(x)$. (ii) Using the chemical exchange (CE) process, we mix GaN and BN on the ordered alloy phase at $V=V(x)$. (iii) In the structural relaxation (SR) step, we relax all atomic positions. Thus, the total optical band-gap bowing is finally: $b=b_{VD}+b_{CE}+b_{SR}$.

At x = 0.25(0.5), we found b_{VD} = 5.2(6.42)eV, b_{CE} = 3.65(6.26)eV, and b_{SR} = 0.05(-1.38)eV, giving a total bowing parameter of 8.9(11.30)eV. The calculated total bowing at x = 0.25 and at x = 0.5 divulge relative strong dependence on B composition. Furthermore, b comes mainly from the structural volume deformation effect and chemical effect (via the charge-exchange); whereas the structural relaxation term b_{SR} is relatively weak compared to b_{VD} and b_{CE}. The b_{CE} term scales with the strong electronegativity mismatch between Ga and B atoms (~12% according to Pauling's scale). However, the volume deformation contribution b_{VD} can be attributed to the large mismatch of the lattice constants a of GaN and BN (~22%).

4 Conclusion

In conclusion, using high-throughput first-principles computational approach, we explored stable ordered phases of GaN-BN alloys. We have uncovered three ordered structures, namely cubic (BGa_3N_4, and B_3GaN_4, space group *P*-43m), and tetragonal ($BGaN_2$, space group *P*-42m). BGa_3N_4 ($BGaN_2$ and B_3GaN_4) are found fairly thermodynamically stable (unstable). All those ordered structures are found to be mechanically and dynamically stable. Interestingly though, it is found that B_3GaN_4 compound exhibits high bulk (328GPa) and shear (248GPa) moduli. In addition, we found that B_3GaN_4 is a potential hard material with Vickers hardness of about ~33GPa. In accord with photoluminescence measurement, state-of-the-art LDA-1/2 approach evinces a giant optical band gap bowing (*b*~11eV) over the entire range of boron composition *x*. Furthermore, *b* is found composition-depend and emerge mainly from chemical (charge exchange) and structural (volume deformation) effects.

References

[1] A. Y. Polyakov, M. Shin, M. Skowronski, D. W. Greve, R. G. Wilson, A. V. Govorkov, and R. M. Desrosiers, Growth of GaBN ternary solutions by organometallic vapor phase epitaxy, J. Electron. Mater. **26** (1997) 237-242. DOI: 10.1007/s11664-997-0157-x

[2] A. Ougazzaden, S. Gautier, C. Sartel, N. Maloufi, J. Martin, F. Jomard, BGaN materials on GaN/sapphire substrate by MOVPE using N2 carrier gas, J. Crystal Growth **298** (2007) 316-319. DOI: 10.1016/j.jcrysgro.2006.10.072

[3] T. Akasaka, Y. Kobayashi, T. Makimoto, BGaN micro-islands as novel buffers for growth of high-quality GaN on sapphire, J. Crystal Growth **298** (2007) 320-324. DOI: 10.1016/j.jcrysgro.2006.10.033

[4] G. Orsal, N. Maloufi, S. Gautier, M. Alnot, A. A. Sirenko, M. Bouchaour, and A. Ougazzaden, Effect of boron incorporation on growth behavior of BGaN/GaN by MOVPE, J. Crystal Growth **310** (2008) 5058-5062. DOI: 10.1016/j.jcrysgro.2008.08.024

[5] A. Ougazzaden, S. Gautier, T. Moudakir, Z. Djebbour, Z. Lochner, S Choi, H. J. Kim, J. – H. Ryou, R. D. Dupuis, and A. A. Sirenko, Bandgap bowing in BGaN thin films, Appl. Phys. Lett. **93** (2008) 083118-083118-3. DOI: 10.1063/1.2977588

[6] A. Said, M. Debbichi, and M. Said, Theoretical study of electronic and optical properties of BN, GaN and BxGa1−xN in zinc blende and wurtzite structures, Optik **127** (2016) 9212-9221. DOI: 10.1016/j.ijleo.2016.06.103

[7] X. Li, S. Wang, H. Liu, F. A. Ponce, T. Detchprohm and R. D. Dupuis,
100-nm thick single-phase wurtzite BAlN films with boron contents over 10: 100-nm thick single-phase wurtzite BAlN films, DOI: 10.1002/pssb.201600699, Phys. Status Solidi B **254** (2017) 1600699.

[8] L. Escalanti, and G. L. W. Hart, Boron alloying in GaN, Appl. Phys. Lett. **84** (2004) 705-707. DOI: 10.1063/1.1644910

[9] K. Liu, H. Sun, F. AlQatari, W. Guo, X. Liu, J. Li, C. G. Torres Castanedo, and X. Li, Wurtzite BAlN and BGaN alloys for heterointerface polarization engineering, Appl. Phys. Lett. **111** (2017) 222106. DOI: 10.1063/1.5008451

[10] T. Akiyama, K. Nakamura, and T. Ito, Effects of lattice constraint on structures and electronic properties of BAlN and BGaN alloys: A first-principles study, Appl. Phys. Express **11** (2018) 025501. DOI: 10.7567/APEX.11.025501

[11] H. Maiz Hadj Ahmed, H; Benaissa, A. Zaoui and M. Ferhat, Exploring new insights in BAlN from evolutionary algorithms *ab initio* computations, Phys. Lett. A 383, 2019, 1385-1388. DOI: 10.1016/j.physleta.2019.02.010

[12] M. Ferhat, Computational optical band gap bowing of III–V semiconductors alloys, phys. stat. sol. (b) **241** (2004) R38-R41. DOI: 10.1002/pssb.200409048

[13] M. Ferhat and F. Bechstedt, First-principles calculations of gap bowing in $InxGa_{1-x}N$ and $In_xAl_{1-x}N$ alloys: Relation to structural and thermodynamic properties, Phys. Rev. B **65** (2002) 075213. https://doi.org/10.1103/PhysRevB.65.075213

[14] A. Belabbes, M. Ferhat and A. Zaoui, Giant and composition-dependent optical band gap bowing in dilute $GaSb_{1-x}N_x$ alloys, Appl. Phys. Lett. **88** (2006) 152109. DOI: 10.1063/1.2196049

[15] H. Benaissa, A. Zaoui, and M. Ferhat, First principles calculations for dilute InAs1−xNx alloys, J. Appl. Phys. **102** (2007) 113712. DOI: 10.1063/1.2821144

[16] A. Belabbes, A. Zaoui and M. Ferhat, Lattice mismatch consequences for the intrinsic characteristics in the dilute (Zn, Se)O alloys, J. Phys.: Condens. Matter **19** (2007) 456212. DOI: 10.1088/0953-8984/19/45/456212

[17] A. Berghout, A. Zaoui, J. Hugel and M. Ferhat, First-principles study of the energy-gap composition dependence of $Zn_{1-x}Be_xSe$ ternary alloys, Phys. Rev. B **75** (2007) 205112. https://doi.org/10.1103/PhysRevB.75.205112

[18] A. Belabbes, A. Zaoui, S. Laref and M. Ferhat, Imposing changes of band and spin–orbit gaps in GaNBi, Solid State Commun **152** (2012). 1700-1702. DOI: 10.1016/j.ssc.2012.04.071

[19] A. Jain, S. P. Ong, G. Hautier, W. Chen, W. D. Richards, S. Dacek, S. Cholia, D. Gunter, D. Skinner, G. Ceder, and K. A. Persson, Commentary: The Materials Project: A materials genome approach to accelerating materials innovation, APL Mater. **1** (2013) 011002 (2013), https://www.materialsproject.org. DOI: 10.1063/1.4812323

[20] G. Hautier, C. Fischer, V. Ehrlacher, A. Jain, and G. Ceder, Data Mined Ionic Substitutions for the Discovery of New Compounds, Inorg. Chem. **50** (2011) 656-663. DOI: 10.1021/ic102031h

[21] W. Kohn and L. J. Sham, Self-Consistent Equations Including Exchange and Correlation Effects, Phys. Rev. **140** (1965) A1133. https://doi.org/10.1103/PhysRev.140.A1133

[22] P. Giannozzi et al., QUANTUM ESPRESSO: a modular and open-source software project for quantum simulations of materials, J. Phys. : Condens. Matter **21** (2009) 395502-395502. DOI: 10.1088/0953-8984/21/39/395502

[23] J. P. Perdew and A Zunger, Self-interaction correction to density-functional approximations for many-electron systems, Phys. Rev. B **23** (1981) 5048. https://doi.org/10.1103/PhysRevB.23.5048

[24] A. Dal Corso, Projector augmented-wave method: Application to relativistic spin-density functional theory, Phys. Rev. B **82** (2010) 075116. https://doi.org/10.1103/PhysRevB.82.075116

[25] H. J. Monkhorst and J. D. Pack, Special points for Brillouin-zone integrations, Phys. Rev. B **13** (1976) 5188. https://doi.org/10.1103/PhysRevB.13.5188

[26] S. Baroni, S. de Gironcoli, A. Dal Corso, and P. Giannozzi, Phonons and related crystal properties from density-functional perturbation theory, Rev. Mod. Phys. **73** (2001) 515. https://doi.org/10.1103/RevModPhys.73.515

[27] X. Q. Che, H. Y. Niu, D. Z. Li, and Y. Y. Li, Modeling Hardness of Polycrystalline Materials and Bulk Metallic Glasses. Intermetallics, Intermetallics, **19** (2011) 1275. http://dx.doi.org/10.1016/j.intermet.2011.03.026

[28] I. Vurgaftman, J. R. Meyer and L. R. Ram-Mohan, Band parameters for III–V compound semiconductors and their alloys, J. Appl. Phys. **89** (2001) 5815, and references therein. DOI: 10.1063/1.1368156

[29] T. Soma, S. Sawaoka, and S. Saito, Characterization of wurtzite type boron nitride synthesized by shock compression, Mater. Res. Bull. **9** (1974) 755. DOI: 10.1016/0025-5408(74)90110-X

[30] A. Polian, M. Grimsditch and I. Grzegory, Elastic constants of gallium nitride J. Appl. Phys. **79** (1996) 3343-3344. DOI: 10.1063/1.361236

[31] K. Kim, W. R. L. Lambrecht, and B. Segall, Elastic constants and related properties of tetrahedrally bonded BN, AlN, GaN, and InN, Phys. Rev. B **53** (1996) 16310. https://doi.org/10.1103/PhysRevB.53.16310

[32] M. E. Sherwin and T. J Drummond, Predicted elastic constants and critical layer thicknesses for cubic phase AlN, GaN, and InN on β-SiC, J. Appl. Phys. **69** (1991) 8423.

[33] L. G. Ferreira, M. Marques, and L. K. Teles, Approximation to density functional theory for the calculation of band gaps of semiconductors, Phys. Rev. B **78** (2008) 125116. https://doi.org/10.1103/PhysRevB.78.125116

[34] M. S. Hybertsen and S. G. Louie, Model dielectric matrices for quasiparticle self-energy calculations, Phys. Rev. B **37** (1988) 2733. https://doi.org/10.1103/PhysRevB.37.2733

[35] S. P. Gao, Cubic, wurtzite, and 4H-BN band structures calculated using GW methods and maximally localized Wannier functions interpolation, Comput. Mater. Sci. **61** (1992) 266. https://doi.org/10.1016/j.commatsci.2012.04.039

[36] M. Zhang and X. Li, Structural and electronic properties of wurtzite BxAl1–xN from first-principles calculations, Phys Status Solidi B **254** (2017) 1600794. https://doi.org/10.1002/pssb.201600749

[37] C. –K. Tan, D. Borovac, W. Sun, and N. Tansu, First-Principle Electronic Properties of Dilute-P GaN1−xPx Alloy for Visible Light Emitters, Scientific Reports **6** (2016) 24412. DOI: 10.1038/srep24412

[38] S. Azzi, A. Zaoui and M. Ferhat, On the importance of the band gap bowing in Boron-based III–V ternary alloys, Solid State Commun **144** (2007) 245, and reference therein. DOI: 10.1016/j.ssc.2007.08.017

[39] J. –X. Shen, D. Wickramaratne, and C. G. Van de Walle, Band bowing and the direct-to-indirect crossover in random BAlN alloys, Phys. Rev. Materials **1** (2017) 065001. https://doi.org/10.1103/PhysRevMaterials.1.065001

[40] J. E. Bernard and A. Zunger, Electronic structure of ZnS, ZnSe, ZnTe, and their pseudobinary alloys, Phys. Rev. B **36** (1987) 3199. https://doi.org/10.1103/PhysRevB.36.3199

Table Captions

Table I: Calculated equilibrium structural parameters, for GaN, BGa_3N_4, $BGaN_2$, B_3GaN_4 and BN.

Table II: Calculated elastic constants (in GPa) of GaN, BGa_3N_4, $BGaN_2$, B_3GaN_4 and BN.

Table III: Calculated bulk modulus B_0 (in GPa), Young's modulus E (in GPa), shear modulus G (in GPa), and Poisson's ratio ν (in GPa).

Figure Captions

Fig. 1: Calculated formation enthalpy of $B_xGa_{1-x}N$ alloys.

Fig. 2: Phonon band structure and phonon density of states of a) BGa_3N_4, b) $BGaN_2$, and c) B_3GaN_4.

Fig. 3: Band-gap dependence of $B_xGa_{1-x}N$ on B composition.

Table I

Phase	*a*(Å)	*c/a*	*Space group*
GaN	3.160 3.189[a]	1.630 1.626[a]	*P*6$_3$mc
BGa$_3$N$_4$	4.240		*P*-43m
BGaN$_2$	2.796	1.500	*P*-4m2
B$_3$GaN$_4$	3.820		*P*-43m
BN	2.525 2.553[b]	1.654 1.656[b]	*P*6$_3$mc

[a]Ref.[28].

[b]Ref.[29].

Table II

	C_{11}	C_{12}	C_{13}	C_{33}	C_{44}
GaN	366	138	101	407	95
Expt.[a]	390	145	106	398	105
BGa$_3$N$_4$	364	172			189
BGaN$_2$	553	67	189		223
B$_3$AGaN$_4$	586	199			293
BN	986	146	65	1097	345
Calc.[b]	987	143	70	1020	369

[a]Ref.[30].

[b]Ref.[31].

Table III

	B_0	E	G	ν
GaN	202(190[a])	284	112	0.26
BGa_3N_4	236	342	144	0.24
$BGaN_2$	279	457	196	0.22
B_3GaN_4	328	596	248	0.19
BN	402(410[a])	908	404	0.12

[a]Ref.[32].

Figure 1

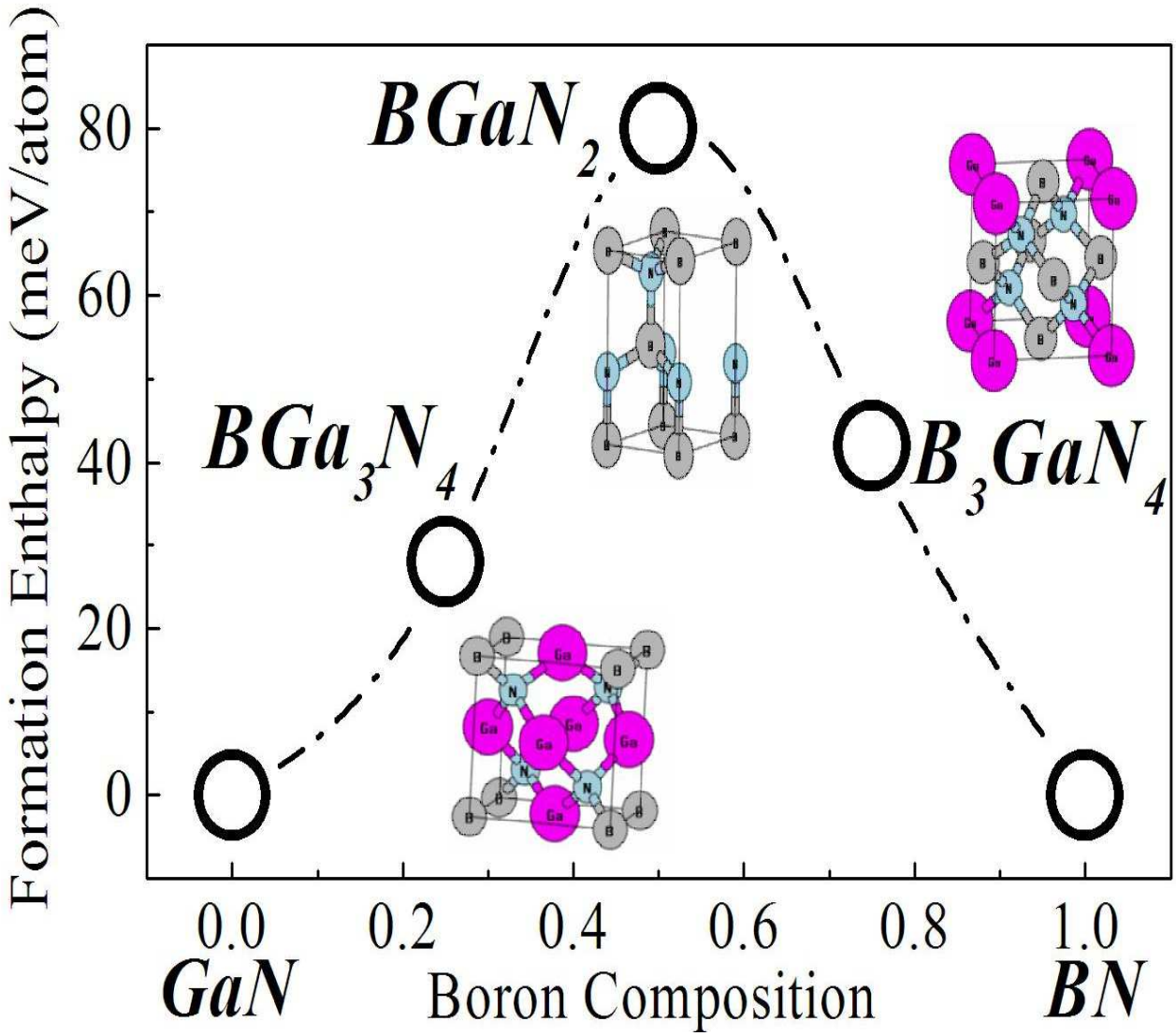
Formation Enthalpy (meV/atom)
80
60
40
20
0
BGaN2
BGa3N4
B3GaN4
0.0
0.2
0.4
0.6
0.8
1.0
GaN
Boron Composition
BN

Figure 2

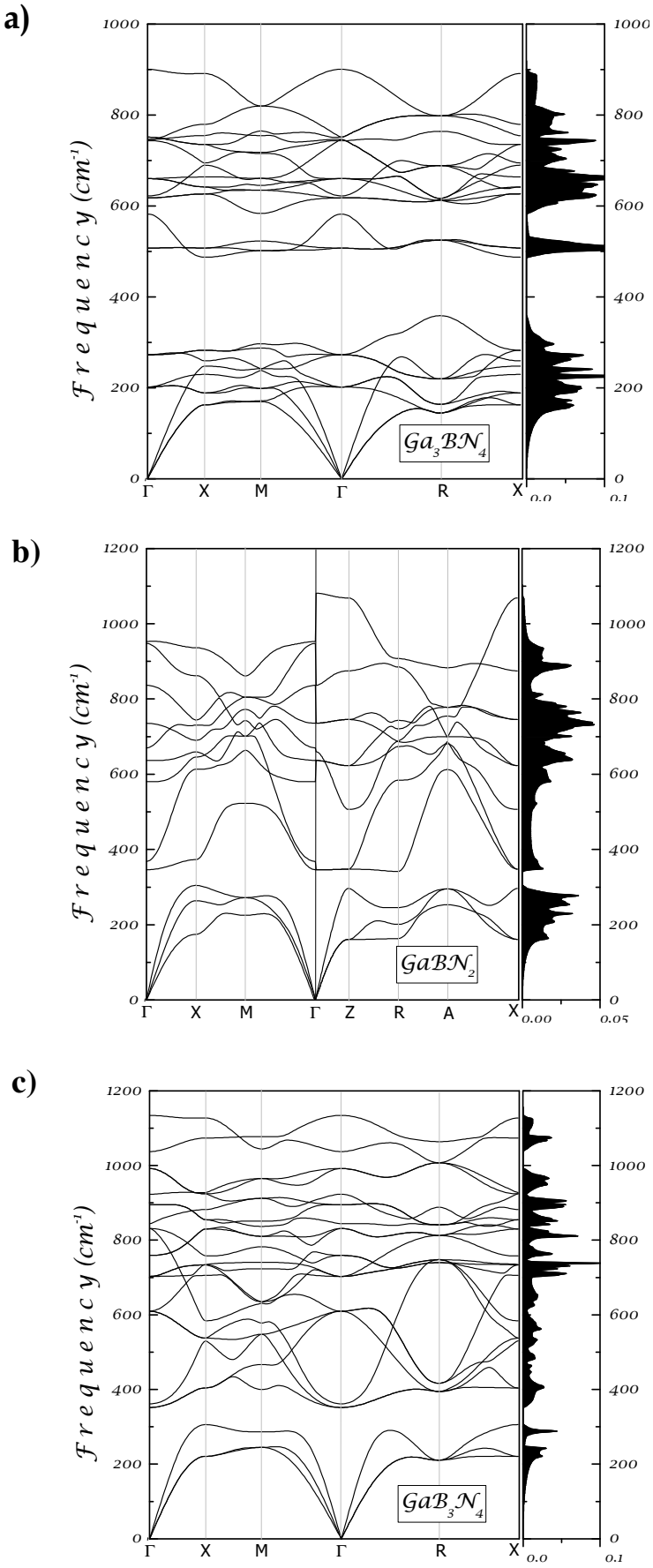
a)
b)
c)
Frequency (cm-1)
Ga3BN4
GaBN2
GaB3N4
Γ X M Γ R X
Γ X M Γ Z R A X
Γ X M Γ R X
0 200 400 600 800 1000 1200
0.0 0.1
0.00 0.05

Figure 3

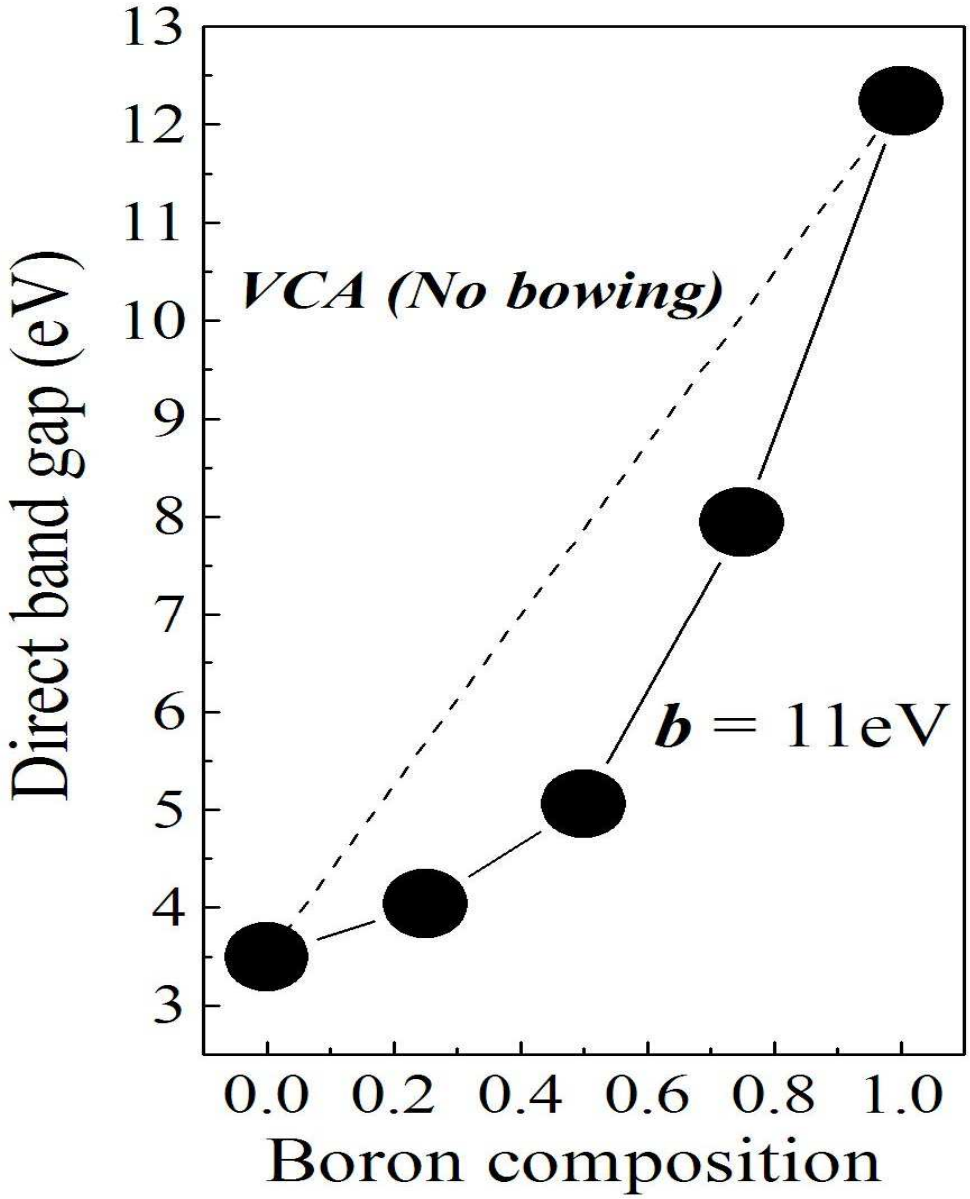
Direct band gap (eV)
13
12
11
10
9
8
7
6
5
4
3
VCA (No bowing)
b = 11eV
0.0
0.2
0.4
0.6
0.8
1.0
Boron composition